

The Optical Diode Ideality Factor Enables Fast Screening of Semiconductors for Solar Cells

Finn Babbe,* Leo Choubrac, and Susanne Siebentritt

In the search for new materials for solar cells, fast feedback is needed. Radiative efficiency measurements based on photoluminescence (PL) are the tool of choice to screen the voltage a material is capable of. Additionally the dependence of the radiative efficiency on excitation density contains information on the diode ideality factor, which determines in turn the fill factor of the solar cell. Both parameters are immediate ingredients of the efficiency of a solar cell and can be determined from PL measurements, which allow fast feedback. The method to determine the optical diode ideality factor from PL measurements and compare to electrical measurements in finished solar cells are discussed.

1. Introduction

A range of materials is currently used and deployed in solar cells.^[1] Yet, an intensive search is going on for new materials, that are more abundant^[2] and that are still at least as energy, materials, and/or cost efficient as the existing materials.^[3] Various criteria have been defined for materials screening based on computational methods.^[4–9] Experimental materials screening^[10] needs feedback from fast measurements, that do not rely on finished devices. Optical measurements based on photoluminescence (PL) allow for a fast screening. A widely used criterion^[11–13] for the suitability of a (new) material for solar cell applications is the radiative efficiency or the quasi Fermi level (qFL) splitting. Both quantities are closely related.^[14–16] They describe the open-circuit voltage an absorber material is capable of, which is a decisive criterion for the efficiency of a solar cell. Another important property with significant influence on the device efficiency is the diode ideality factor. From the diode characteristics under illumination we can derive the dependence of the open circuit voltage

(see e.g., ref. [17]) $e \cdot V_{oc} = E_{rec} - AkT \ln(j_{00}/j_{ph})$, where V_{oc} is the open circuit voltage, e is the elemental charge, E_{rec} is the activation energy, A is the diode ideality factor, k is the Boltzmann's constant, T is the temperature, j_{ph} is the photocurrent of the solar cell and j_{00} is the prefactor of the reverse saturation current. The higher the diode ideality factor the lower the open circuit voltage becomes at room temperature or at operating temperature. Furthermore, the fill factor of a solar cell depends critically on the diode ideality factor^[18] (besides, of course, the resistances and the saturation current). The diode factor of a finished solar cell depends on

many factors, determined by the absorber or the interfaces. In developing new materials for solar cells it is, thus, important to know whether optimization is needed mostly for the absorber or mostly for the interfaces.

Therefore, in both; the experimental screening of new materials and the development of new materials into solar cells a quality control of the absorber itself is needed. This can be provided by PL measurements, which also can give information on the diode ideality factor. The diode ideality factor is originally defined by the current-voltage (jV) characteristics of a diode $j = j_0(\exp(eV/kT) - 1)$, with current density j , reverse saturation current j_0 , unit charge e , the applied voltage V , Boltzmann constant k , temperature T and diode ideality factor A . The diode ideality factor depends on the dominating recombination mechanism.^[19,20] It can be determined from the slope of the logarithm of the forward current with applied bias. The forward current in any p-n diode involves necessarily a recombination process, since the current on the n-side of the diode is carried by electrons, whereas on the p-side it is carried by holes.^[21] The classical model by Shockley^[21] considers injection of minority carriers through the space charge region which then recombine outside the space charge region within the distance of the diffusion length. Thereby it is not important whether the recombination takes place radiatively or non-radiatively. The diode ideality factor in this case is 1. The other classical example is Shockley-Read-Hall recombination in the space charge region through a defect at mid-gap, where the diode ideality factor becomes 2.^[22] Descriptively this can be understood by the voltage drop being split into half for the path of the electrons and half for the path of the holes.^[19] Another way to look at it is that both the quasi Fermi level (qFL) of the electrons and of the holes move symmetrically to the defect with changing applied voltage.^[20] In a hetero

F. Babbe, Prof. S. Siebentritt
Laboratory for Photovoltaics
Physics and Materials Science Research Unit
University of Luxembourg
41 Rue de Brill, 4422 Belvaux, Luxembourg
E-mail: finn.babbe@uni.lu

Dr. L. Choubrac
Department Structure and Dynamics of Energy Materials
Helmholtz-Zentrum Berlin
Hahn-Meitner-Platz 1, 14109 Berlin, Germany

 The ORCID identification number(s) for the author(s) of this article can be found under <https://doi.org/10.1002/solr.201800248>.

DOI: 10.1002/solr.201800248

junction, the recombination at the interface can dominate with a diode ideality factor given by the ratio of the voltage drops on either side^[23] or a diode ideality factor of 1, when the Fermi level is pinned.^[24] For a detailed discussion see ref. [20,25]. Thus, the diode ideality factor is closely related to the details of the electronic structure of the complete device.

The recombination taking place in the bulk of the semiconductor can be monitored by luminescence studies. Although luminescence is obviously based on radiative transitions, information on non-radiative recombination is obtained from the intensity and its dependence on excitation. PL experiments can be performed on the semiconductor film without finishing the device structure and the excitation can be precisely controlled by the intensity of the laser source. The result of an excitation dependent measurement series is usually the observation of a power law dependency that stretches over several orders of magnitude according to:

$$I_{\text{PL}} \sim I_{\text{laser}}^b \quad (1)$$

with I_{PL} the integrated PL intensity, I_{laser} the intensity of the excitation and b the exponent. Room temperature PL is typically dominated by band-band recombination, that is, the recombination of free electrons in the conduction band with free holes in the valence band. If there are no other recombination channels, the luminescence increases linearly with the excitation and $b = 1$ (see e.g., Spindler).^[26–29] If competing channels exist however, in particular those involving defects in the band gap, the exponent will be higher than 1.^[26–28]

PL^[30–34] has been used in the past to study and predict the role of different recombination channels in the finished devices for various solar technologies. But these studies had a different purpose than our study. In several investigations the measurements were performed on finished solar cells^[30,31,35] or the goal was to determine the recombination activity of grain boundaries^[33] or the radiative recombination coefficient.^[34] In another study^[32] an approach similar to ours was used to differentiate between bulk and interface recombination. Below we also discuss this distinction but go beyond in predicting the diode ideality factor of the finished device from the PL measurement of the absorber covered with the buffer layer alone. A similar approach has been used for Si wafer,^[36] but in the presented study we extend this method to analyze the cell formation process and determine the performance limiting interface or layer. We will discuss how the exponent b of the PL power law relates to the diode ideality factor of the finished device. We use thin film solar cells based on a Cu(In,Ga)Se₂ absorber layers as an example. Currently, they reach the highest efficiencies of any thin film technology on rigid substrates,^[37] as well as on flexible substrates.^[38] For the current study they are particularly interesting since within one material class using the same preparation method we can have devices that are dominated by recombination in the bulk, when we use a Cu-poor absorber, or by recombination at or near the interface, when we use absorbers grown under Cu-excess.^[39,40]

1.1. Luminescence, Voltage, and Current

The radiative recombination rate R^{rad} in a semiconductor is given by Planck's generalized law,^[16,41] which can generally be simplified to^[42]

$$R^{\text{rad}} = R_0 \cdot \exp(e\mu/kT) \quad (2)$$

where R_0 is the equilibrium recombination rate that balances the thermal radiation^[43,44] and μ is the qFL splitting.

In the case where radiative band-band recombination is the only recombination path we get,

$$I_{\text{laser}} \propto G = R = R^{\text{rad}} \propto I_{\text{PL}} \quad (3)$$

since the recombination rate R must balance the generation rate G . Equation (3) is the same as Equation (1) with $b = 1$, as discussed above for the case where band–band recombination is the sole recombination channel.

In the case where competing recombination channels exist we get from Equations (1) and (2)

$$R^{\text{rad}} \propto G^b \propto R_0 \exp(e\mu/kT) \quad (4)$$

To relate this with the jV characteristics of the device under illumination we assume that we can neglect parasitic resistances. To compare with the situation of the PL measurement, which is always under open circuit condition, we can write:

$$j_{\text{ph}} = j_0(\exp(eV_{\text{OC}}/kT) - 1) \approx j_0 \cdot \exp(eV_{\text{OC}}/kT) \quad (5)$$

with the photocurrent j_{ph} and the open circuit voltage V_{OC} . If we now take into account that the photocurrent is given the illumination and thus by the generation rate, we can use Equation (4) and write:

$$j_{\text{ph}} \sim G \sim \exp(e\mu/bkT) \quad (6)$$

Comparing Equations (5) and (6) we see that the diode ideality factor of the finished device is directly given by the exponent of the PL power law under the following conditions: 1) we can equate $\mu = V_{\text{OC}}$. This is generally the case if the qFL splitting is measured as a spatial average,^[45] 2) the finishing of the device with adding contacts and interfaces does not add new recombination channels. This is something that has to be checked experimentally. In the case where the above conditions are fulfilled, the diode ideality factor of the finished device is already determined by the exponent of the power law. We call this exponent the optical diode ideality factor.

2. Experimental Findings

In the following we put this optical diode ideality factor to an experimental check. Illumination dependent PL measurements are carried out at room temperature on a total of five samples with Cu-poor composition as well as four samples that were grown Cu-rich (see section 4). From the calibrated measurements the qFL splitting is extracted. The samples measured are

etched and covered with cadmium sulfide (CdS) to passivate the absorber surface. This passivation is needed since the luminescence yield of bare absorbers degrades by more than a decade within minutes exposed to oxygen and laser illumination,^[46,47] inhibiting illumination dependent measurements. Using the passivated absorber to investigate the properties of the bare absorber is legitimate since the PL properties (peak shape, peak position, and luminescence yield) are the same in freshly etched absorber layers and absorber layer covered with CdS.^[47] That there is no change although the buffer partly forms a junction can be explained by the assumption that the observed PL stems from recombination from the notch of the gallium gradient^[48] see also discussion later in the manuscript. The data of one exemplary Cu-poor sample and on typical Cu-rich sample with similar bandgaps is plotted semi-logarithmically over the excitation density in **Figure 1**. The qFLs increases linearly with excitation in both samples and is about 120 meV higher in the Cu-poor sample than in the Cu-rich sample, as already shown elsewhere.^[47] The slope of the qFLs increase is on average $s = (75 \pm 3)$ meV/decade for Cu-poor samples. Averaging the Cu-rich samples gives a comparable but slightly lower value for s of (69 ± 3) meV/decade.

This slope s can be linked to the power law dependency factor b , when the Equation (1) is inserted into Planck's generalized law shown in Equation (2). From this it is derived that the slope is defined by Equation (7). The prefactor 2.3 is needed to correct for the change from the natural logarithm (in the calculation) to the decadic logarithm used for plotting.

$$s = 2.3 \cdot kT/e \cdot b \quad (7)$$

To verify this relationship the qFL splitting was measured on a broad range of CIGS absorber layers covered with CdS as well as on finished devices. The gallium content was varied from no to considerable high amounts ($0 < [\text{Ga}]/([\text{Ga}]+[\text{In}]) < 0.4$). The copper content was varied between 0.8 and 1.4 ($0.8 < [\text{Cu}]/([\text{Ga}]+[\text{In}]) < 1.4$). For the extraction of the power law

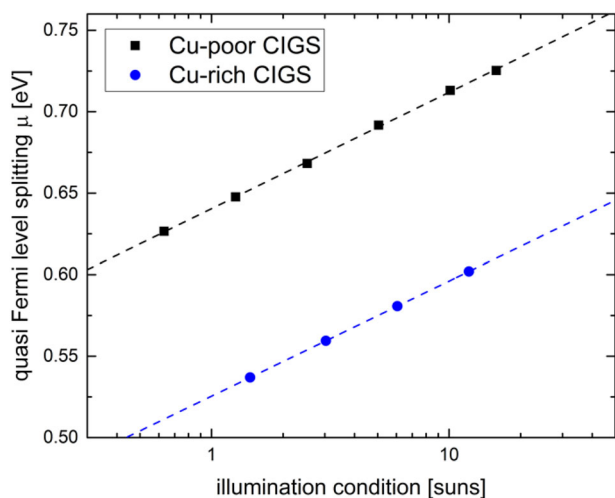


Figure 1. Quasi Fermi level splitting measured at room temperature for a Cu-poor and a Cu-rich grown sample plotted over the equivalent illumination used for excitation.

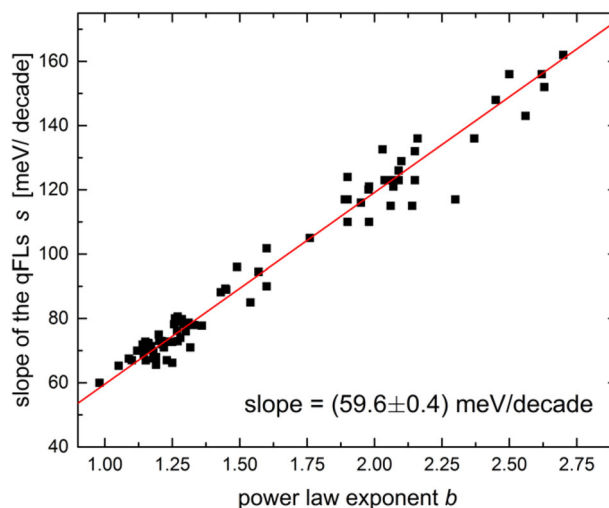


Figure 2. Slope of the qFLs increase with excitation s plotted over the exponent b of the power law from Equation (1). The red line depicts a linear fit.

exponent b , the PL yield was determined by integrating the measured spectra and plotting the yield double-logarithmically over the excitation. The slope of a linear fit through the data defines the b -value.^[49] The slope of the qFLs (s) is plotted over the exponent b in **Figure 2** for all measured samples. It should be noted here that the determination of b yields an at least ten times smaller error than the determination of s , leading to an error mainly in direction of the s -axis in **Figure 2**.

The slope s increases linearly with exponent b . From Equation (7) a slope of (58.7 ± 0.4) meV/decade is expected at the measured room temperature (296 ± 2) K. The linear fit through the data, shown in red, has a slope of (59.6 ± 0.4) meV/decade confirming the relation between the power law exponent and the increase of the qFLs with illumination.

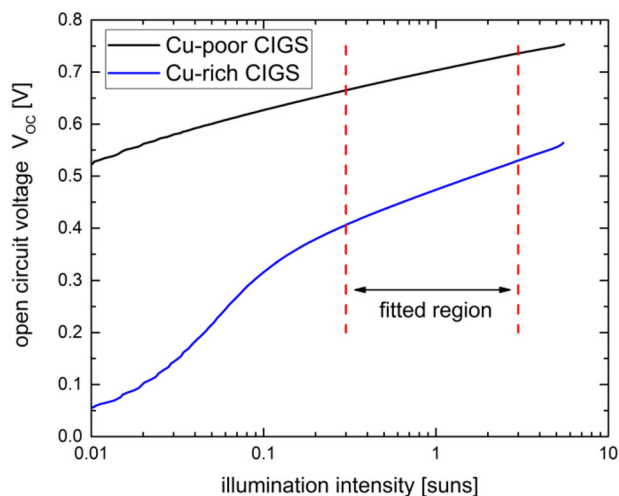


Figure 3. Open circuit voltage of a Cu-poor (black) and Cu-rich (blue) solar cell plotted semi-logarithmically over the illumination conditions during a SunsVoc measurement. The dashed red lines indicate the area fitted for the extraction of the diode ideality factor.

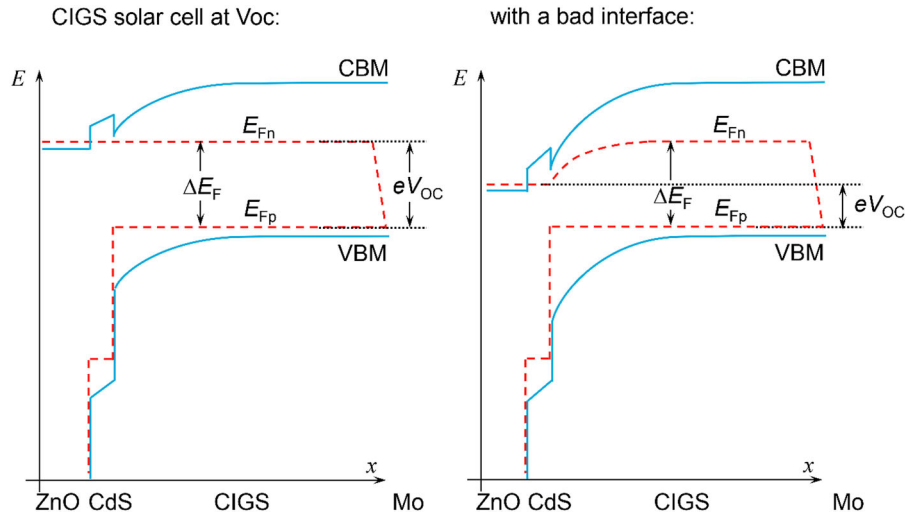


Figure 4. Schematic and simplified band diagram of a CIGS solar cell at open circuit condition. The left side depicts the ideal case, whereas the right side depicts a case with a “bad” interface with a considerably high recombination velocity. For simplicity we assume that the qFLs within the absorber is not influence by the surface recombination. Even in this case, the open circuit voltage would be considerably lower than the qFLs of the absorber itself.

For the smaller set of samples discussed earlier the found relation stated in Equation (7) also holds true. For samples with a Cu-poor composition an average exponent b of (1.25 ± 0.05) and a slope s of (75 ± 3) meV/decade is determined. The average values for the Cu-rich samples are with $b = (1.16 \pm 0.05)$ and $s = (69 \pm 3)$ meV/decade a bit lower but comparable to the Cu poor values.

Each cell of the finished devices is measured under the illumination of a flash lamp in a SunsVoc set up. In **Figure 3** the measured V_{OC} is plotted semi-logarithmically over the illumination for a typical Cu-poor device (black) and a typical Cu-rich (blue) device. The Cu-poor device shows a linear behavior over a wide illumination range. Below 0.1 suns it slightly bends of due to the influence of the shunt resistance. The V_{OC} of the Cu-rich device has a pronounced drop toward low illumination conditions due a very low shunt resistance.^[50] The data for all devices is fitted linearly symmetrically around one sun illumination over one order of magnitude. From the linear fit the slope of the VOC gain, called r in the following, is extracted

Averaging all 29 solar cells with Cu-poor composition a slope r of (80 ± 12) mV/decade and a diode ideality factor of (1.3 ± 0.2) is determined. The diode ideality factor is in good agreement with the previously determined power law exponent (1.25), proving the direct correlation of both properties shown in theory. Thus the power law exponent can be defined as optical diode ideality factor. It should be noted here, that for the extraction of the optical diode factor from intensity dependent PL measurements the set up does not need to be calibrated or the qFLs to be extracted. The optical diode factor is given by the slope of a linear fit of the PL intensity over the excitation density in a double logarithmic plot. The absolute calibration of the luminescence yield (multiplicative factor) and the calibration of the excitation density (multiplicative factor) only shift the data in such a plot, but does not change the slope. This makes this property easy to access in all PL set ups in which the excitation density can be varied.

The samples grown under Cu-excess (averaging 26 cells) exhibit a larger slope r of (112 ± 9) mV/decade leading to an average diode ideality factor of (1.9 ± 0.2) . This value is well above the determined power law exponent of (1.15). The higher diode factor matches the values found for Cu-rich CuInSe₂ solar cells^[48] and can be explained by the fact that Cu-rich solar cells are dominated by recombination close to the interface.^[40,51] This has also been shown for the here used Cu-rich samples by temperature dependent current voltage measurements (see supplementary materials of ref. [47]). The mismatch can be thus explained by an additional recombination channel created during device finishing.

For both compositions we probe the qFLs inside the absorber layer which is essentially a bulk property. In the ideal case, device finishing does not add recombination channels. Then the bulk qFLs and the open circuit voltage at the terminals is the same as indicated on the left side of **Figure 4**. When another recombination path is added due to a “bad” interface with a high recombination velocity the qFLs splitting decreases toward the terminals, as depicted on the right side of **Figure 4**, leading not only to a reduction of V_{OC} but also changing diode factor. The comparison of the diode factor and the optically diode factor can be used to unveil those bad interfaces, which limit the device performance.

3. Conclusion

We have shown, that the power law exponent b of the PL of a solar cell absorber is directly linked to the diode ideality factor A of the completed device. If the device is dominated by recombination in the bulk of the absorber, the power law exponent and the diode ideality factor agree. If additional recombination channels are present in the finished device, like interface recombination, the diode factor of the finished device is larger than the power law

exponent. The approach was confirmed using Cu(In,Ga)Se₂ solar cells, which have the advantage that different recombination channels are present and can be controlled in the solar cells of the same class of absorbers.

The approach is relevant for the screening of new materials for solar cells, since it allows a quick measurement of the diode ideality factor, which has implications for the fill factor of the solar cell, before finishing the device, based on the PL of the absorber alone. The approach can furthermore be used in for the development of new materials into solar cells as it indicates whether the limitations of the solar cell stem from the absorber or from the interface and thus indicates in which direction optimisation efforts need to be directed.

4. Experimental Section

Polycrystalline CIGS samples are grown by a 3-stage evaporation process on glass substrates covered with molybdenum in a molecular beam epitaxy system (details can be found elsewhere).^[52,53] The Indium flux is varied to achieve [Ga]/([Ga]+[In]) ratios (GGI) between 0.25 and 0.4. The length of the third stage is varied to control the final [Cu]/([Ga]+[In]) ratio (CGI). Samples with a long 3rd stage exhibit an overall CGI of 0.9, measured by energy dispersive X-ray spectroscopy (EDX). They will be called Cu-poor within the script. Samples grown with a short 3rd stage exhibit an overall CGI of about 1.2, due to secondary Cu_xSe phases on top of a stoichiometric bulk. After growth, those secondary phases are removed by a 5 min etching in a 10% aqueous potassium cyanide solution (KCN). Although the absorbers are stoichiometric after etching, they will be called Cu-rich for easy differentiation between the two sample sets. The Cu-poor samples are also etched in 5% aqueous KCN solution for 30 s to remove residual oxides.^[51,54] After etching, the absorber layers are covered by a 40 nanometer thin CdS layer applied by chemical bath deposition. A small piece is cut from the absorber after CdS deposition for PL measurements. The remaining absorber is finished by a sputtered intrinsic zinc oxide and aluminium doped zinc oxide double layer as well as nickel aluminium grids.

The PL properties are measured in a home built set up under continuous illumination from a diode laser (660 nanometer wavelength). The emitted PL is collected by an off-axis mirror and focused into a fiber by a second off-axis mirror. The light is afterwards split by a grating monochromator and detected by a detector array (Si or InGaAs). For the evaluation of the qFL splitting and the calibration steps refer to literature.^[16,47,49] For the determination of the diode ideality factor of the finished cells, SunsVoc measurements are carried out in a Sinton Instruments system.^[55,56] With this method, the V_{OC} is measured over a wide range of illumination intensities during the flash of a xenon lamp (12 ms). The diode ideality factor is extracted by a linear fit of the V_{OC} plotted semi-logarithmically over the illumination. This method has the advantage that it is not disturbed by the series resistance. This measurement technique is well known in the silicon community^[55,56] but has also successfully employed for CIGS^[57] and kesterite^[57] cells. Furthermore, there is a great correspondence between the illumination dependent V_{OC} measurements for the extraction of the diode ideality factor on the one side, and the illumination dependent PL measurements for the extraction of the qFLs and the exponent *b* of the power law on the other side.

Acknowledgements

This contribution has been funded by the Luxembourgish Fonds National de la Recherche (FNR) in the framework of the CURI-K project which is gratefully acknowledged. The authors gratefully thank the DLR Institute of

Networked Energy Systems (formerly Next Energy) (Oldenburg, Germany) for the possibility to use their SunsVoc set up.

Conflict of Interest

The authors declare no conflict of interest.

Keywords

diode factor, material screening, photoluminescence, SunsVoc

Received: September 6, 2018

Revised: October 1, 2018

Published online:

- [1] A. Polman, M. Knight, E. C. Garnett, B. Ehrler, W. C. Sinke, *Science* **2016**, 352, aad4424.
- [2] C. Wadia, A. P. Alivisatos, D. M. Kammen, *Environ. Sci. Technol.* **2009**, 43, 2072.
- [3] N. M. Haegel, R. Margolis, T. Buonassisi, D. Feldman, A. Froitzheim, R. Garabedian, M. Green, S. Glunz, H.-M. Henning, B. Holder, I. Kaizuka, B. Kroposki, K. Matsubara, S. Niki, K. Sakurai, R. A. Schindler, W. Tumas, E. R. Weber, G. Wilson, M. Woodhouse, S. Kurtz, *Science (80-)*. **2017**, 356, 141.
- [4] L. Yu, A. Zunger, *Phys. Rev. Lett.* **2012**, 108, 068701.
- [5] J. Hachmann, R. Olivares-Amaya, A. Jinich, A. L. Appleton, M. A. Blood-Forsythe, L. R. Seress, C. Román-Salgado, K. Trepte, S. Atahan-Evrenk, S. Er, S. Shrestha, R. Mondal, A. Sokolov, Z. Bao, A. Aspuru-Guzik, *Energy Environ. Sci.* **2014**, 7, 698.
- [6] R. E. Brandt, V. Stevanović, D. S. Ginley, T. Buonassisi, *MRS Commun.* **2015**, 5, 265.
- [7] K. T. Butler, J. M. Frost, J. M. Skelton, K. L. Svane, A. Walsh, *Chem. Soc. Rev.* **2016**, 45, 6138.
- [8] B. Blank, T. Kirchartz, S. Lany, U. Rau, *Phys. Rev. Appl.* **2017**, 8, 024032.
- [9] T. Kirchartz, U. Rau, *Adv. Energy Mater.* **2018**, 1703385, 1703385.
- [10] A. J. Lehner, D. H. Fabini, H. A. Evans, C.-A. Hébert, S. R. Smock, J. Hu, H. Wang, J. W. Zwanziger, M. L. Chabinyr, R. Seshadri, *Chem. Mater.* **2015**, 27, 7137.
- [11] H. Sugimoto, M. Tajima, *Jpn. J. Appl. Phys.* **2007**, 46, L339.
- [12] A. D. Collord, H. Xin, H. W. Hillhouse, *IEEE J. Photovoltaics* **2015**, 5, 288.
- [13] S. Almosni, A. Delamarre, Z. Jehl, D. Suchet, L. Cojocar, M. Giteau, B. Behaghel, A. Julian, C. Ibrahim, L. Taty, H. Wang, T. Kubo, S. Uchida, H. Segawa, N. Miyashita, R. Tamaki, Y. Shoji, K. Yoshida, N. Ahsan, K. Watanabe, T. Inoue, M. Sugiyama, Y. Nakano, T. Hamamura, T. Toupance, C. Olivier, S. Chambon, L. Vignau, C. Geoffroy, E. Cloutet, G. Hadziioannou, N. Cavassilas, P. Rale, A. Cattoni, S. Collin, F. Gibelli, M. Paire, L. Lombez, D. Aureau, M. Bouttemy, A. Etcheberry, Y. Okada, J.-F. Guillemoles, *Sci. Technol. Adv. Mater.* **2018**, 19, 336.
- [14] G. Lasher, F. Stern, *Phys. Rev.* **1964**, 133, A553.
- [15] R. T. Ross, *J. Chem. Phys.* **1967**, 46, 4590.
- [16] P. Würfel, *J. Phys. C Solid State Phys.* **1982**, 15, 3967.
- [17] D. Abou-Ras, T. Kirchartz, U. Rau, *Advanced Characterization Techniques for Thin Film Solar Cells*. Wiley-VCH Verlag GmbH & Co. KGaA, Weinheim, Germany **2016**.
- [18] M. A. Green, *Solid. State. Electron.* **1981**, 24, 788.
- [19] S. M. Sze, K. K. Ng, M. S. Sze, K. K. Ng, *Physics of Semiconductor Devices*. John Wiley & Sons, Inc, Hoboken, NJ, USA **2006**.
- [20] R. Scheer, H.-W. W. Schock, *Chalcogenide Photovoltaics*. Wiley-VCH Verlag GmbH & Co. KGaA, Weinheim, Germany **2011**.

- [21] W. Shockley, *Bell Syst. Tech. J.* **1949**, *28*, 435.
- [22] C. Sah, R. Noyce, W. Shockley, *Proc. IRE* **1957**, *45*, 1228.
- [23] U. Dolega, *Zeitschrift Für Naturforsch. A* **1963**, *18*, 653.
- [24] A. Rothwarf, L. C. Burton, J. Hadley, H. C., G. M. Storti, *Photovolt. Spec. Conf. 11th, Scottsdale, Ariz., May 6-8, 1975, Conf. Rec. (A76-14727 04-44) New York, Inst. Electr. Electron. Eng. Inc., 1975*, pp. 476–481. **1975**, 476.
- [25] A. L. Fahrenbruch, R. H. Bube, R. V. D'Aiello, *Fundamentals of Solar Cells (Photovoltaic Solar Energy Conversion)*. Academic Press, New York **1983**.
- [26] T. Schmidt, K. Lischka, W. Zulehner, *Phys. Rev. B* **1992**, *45*, 8989.
- [27] W. Grieshaber, E. F. Schubert, I. D. Goepfert, R. F. Karlicek, M. J. Schurman, C. Tran, *J. Appl. Phys.* **1996**, *80*, 4615.
- [28] M. A. Reshchikov, R. Y. Korotkov, *Phys. Rev. B* **2001**, *64*, 115205.
- [29] C. Spindler, G. Rey, T. Galvani, L. Wirtz, S. Siebentritt, *Submitt. to Phys. Rev. B* **2017**.
- [30] M. Pawlowski, P. Zabierowski, R. Bacewicz, H. Marko, N. Barreau, *Thin Solid Films* **2011**, *519*, 7328.
- [31] L. Lombez, M. Soro, A. Delamarre, N. Naghavi, N. Barreau, D. Lincot, J. F. Guillemoles, *J. Appl. Phys.* **2014**, *116*, 064504.
- [32] V. Sarritzu, N. Sestu, D. Marongiu, X. Chang, S. Masi, A. Rizzo, S. Colella, F. Quochi, M. Saba, A. Mura, G. Bongiovanni, *Sci. Rep.* **2017**, *7*, 1.
- [33] H. C. Sio, T. Trupke, D. Macdonald, *J. Appl. Phys.* **2014**, *116*, 244905.
- [34] T. Trupke, M. A. Green, P. Würfel, P. P. Altermatt, A. Wang, J. Zhao, R. Corkish, *J. Appl. Phys.* **2003**, *94*, 4930.
- [35] Z. Hameiri, P. Chaturvedi, K. R. McIntosh, *Appl. Phys. Lett* **2013**, *103*, 023501.
- [36] T. Trupke, R. A. Bardos, M. D. Abbott, J. E. Cotter, *Appl. Phys. Lett.* **2005**, *87*, 093503.
- [37] http://www.solar-frontier.com/eng/news/2017/1220_press.html, **2017**.
- [38] A. Chirilă, S. Buecheler, F. Pianezzi, P. Bloesch, C. Gretener, A. R. Uhl, C. Fella, L. Kranz, J. Perrenoud, S. Seyrling, R. Verma, S. Nishiwaki, Y. E. Romanyuk, G. Bilger, A. N. Tiwari, *Nat. Mater.* **2011**, *10*, 857.
- [39] S. Siebentritt, L. Gütay, D. Regesch, Y. Aida, V. Deprédurand, *Sol. Energy Mater. Sol. Cells* **2013**, *119*, 18.
- [40] M. Turcu, O. Pakma, U. Rau, *Appl. Phys. Lett.* **2002**, *80*, 2598.
- [41] P. Würfel, *Physics of Solar Cells*. Wiley-VCH Verlag GmbH, Weinheim, Germany **2005**.
- [42] L. Gütay, G. H. Bauer, *Thin Solid Films* **2009**, *517*, 2222.
- [43] H. J. Queisser, *Solid. State. Electron.* **1962**, *5*, 1.
- [44] W. van Roosbroeck, W. Shockley, *Phys. Rev.* **1954**, *94*, 1558.
- [45] A. Delamarre, M. Paire, J.-F. Guillemoles, L. Lombez, *Prog. Photovoltaics Res. Appl.* **2015**, *23*, 1305.
- [46] D. Regesch, L. Gütay, J. K. Larsen, V. Deprédurand, D. Tanaka, Y. Aida, S. Siebentritt, *Appl. Phys. Lett.* **2012**, *101*, 112108.
- [47] F. Babbe, L. Choubrac, S. Siebentritt, *Appl. Phys. Lett.* **2016**, *109*, 082105.
- [48] M. H. Wolter, B. Bissig, E. Avancini, R. Carron, S. Buecheler, P. Jackson, S. Siebentritt, *IEEE J. Photovoltaics* **2018**, *8*, 1320.
- [49] T. Unold, L. Gütay, in *Adv. Charact. Tech. Thin Film Sol. Cells* (Eds: D. Abou-Ras, T. Kirchartz, U. Rau), Wiley-VCH Verlag GmbH & Co. KGaA, Weinheim, Germany **2011**, p. 151.
- [50] F. W. Fecher, A. Pérez Romero, C. J. Brabec, C. Buerhop-Lutz, *Sol. Energy* **2014**, *105*, 494.
- [51] V. Deprédurand, D. Tanaka, Y. Aida, M. Carlberg, N. Fèvre, S. Siebentritt, *J. Appl. Phys.* **2014**, *115*, 044503.
- [52] A. M. Gabor, J. R. Tuttle, D. S. Albin, M. A. Contreras, R. Noufi, A. M. Hermann, *Appl. Phys. Lett.* **1994**, *65*, 198.
- [53] L. Choubrac, T. Bertram, H. Elanzeery, S. Siebentritt, *Phys. Status Solidi* **2017**, *214*, 1600482.
- [54] Y. Hashimoto, N. Kohara, T. Negami, M. Nishitani, T. Wada, *Jpn. J. Appl. Phys.* **1996**, *35*, 4760.
- [55] R.A. Sinton, A. Cuevas, in *16th Eur. Photovolt. Sol. Energy Conf.*, **2000**, 1152.
- [56] M. J. Kerr, A. Cuevas, R. A. Sinton, *J. Appl. Phys.* **2002**, *91*, 399.
- [57] O. Gunawan, T. Gokmen, D. B. Mitzi, *J. Appl. Phys.* **2014**, *116*, 084504.